LAWRENCE
LIVERMORE
NATIONAL
LABORATORY

LLNL-PROC-837638

Evolution of collectivity in 126,128Xe studied in Coulomb excitation measurements

S. Kisyov, C. Y. Wu, J. Henderson, A. Gade, K. Kaneko, Y. Sun, N. Shimizu, T. Mizusaki, D. Rhodes, S. Biswas, A. Chester, M. Delvin, P. Farris, A. Hill, J. Li, E. Rubino, D. Weisshaar

July 19, 2022

15th International Conference on Nuclear Data for Science and Technology (ND2022)
Sacramento (virtual event), CA, United States
July 21, 2022 through July 29, 2022

Disclaimer

Evolution of collectivity in ^{126,128}Xe studied in Coulomb excitation measurements

Stanimir Kisyov[1,*], *Ching-Yen* Wu[1], *Jack* Henderson[2], *Alexandra* Gade[3,4], *Kazunari* Kaneko[5], *Yang* Sun[6], *Noritaka* Shimizu[7], *Takahiro* Mizusaki[8], *Daniel* Rhodes[3,4,**], *Sayani* Biswas[3], *Aaron* Chester[3], *Matthew* Devlin[9], *Peter* Farris[3], *Ava M.* Hill[3], *Jing* Li[3], *Elizabeth* Rubino[3], and *Dirk* Weisshaar[3]

[1]Lawrence Livermore National Laboratory, Livermore, California 94550, USA
[2]Department of Physics, University of Surrey, Guildford, Surrey GU2 7XH, United Kingdom
[3]National Superconducting Cyclotron Laboratory, Michigan State University, East Lansing, Michigan 48824, USA
[4]Department of Physics and Astronomy, Michigan State University, East Lansing, Michigan 48824, USA
[5]Department of Physics, Kyushu Sangyo University, Fukuoka 813-8503, Japan
[6]School of Physics and Astronomy, Shanghai Jiao Tong University, Shanghai 200240, China
[7]Center for Computational Sciences, University of Tsukuba, 1-1-1, Tennodai Tsukuba, Ibaraki 305-8577, Japan
[8]Institute of Natural Sciences, Senshu University, Tokyo 101-8425, Japan
[9]Los Alamos National Laboratory, Los Alamos, NM 87545, USA

Abstract. The characteristics of ^{126,128}Xe were investigated in Coulomb excitation measurements performed at the National Superconducting Cyclotron Laboratory (NSCL) Re-accelerator facility, ReA3, Michigan State University (MSU). The Xe nuclei were accelerated to sub-barrier energies and were impinged on ^{196}Pt and ^{208}Pb targets in separate experimental runs. The scattered nuclei and the de-excitation γ-rays were detected using the JANUS setup. Electromagnetic matrix elements were extracted from the experimental data with the help of the GOSIA/GOSIA2 codes. The results were compared to schematic Davydov-Filippov γ-rigid rotor theoretical calculations and large-scale calculations within a newly-established microscopic shell model (called PMMU model). The experimental results agree well with the theoretical predictions, except for the quadrupole moments of the second 2^+ states in both nuclei, therefore challenging the interpretation of the γ-bands structure.

1 Introduction

The experimental properties of many nuclei in the stable even-*A* Xe mass region suggest a transitional behavior and a certain degree of triaxiality. The exhibit of such characteristics seems to be straight forward given the spherical features of the Sn nuclei and the expected changes when moving towards the mid-shell region.

Non-axially symmetric shapes can be related both to two extreme phenomenological models: (1) the γ-rigid rotor model of Davydov and Flippov (DF) [1] and (2) the γ-soft model of Wilets and Jean (WJ) [2] (which is also closely related to the O(6) dynamical symmetry of the Interacting Boson Model).

Recent works on the even-*A* Xe isotopes consider ^{128}Xe as a possible E(5) critical point in the transition from spherical to O(6)-structure γ-soft nuclei [3], while other studies [4] suggest that ^{130}Xe is the most likely candidate for E(5) among the Xe isotopes. Deviations from the O(6) predictions for certain transition strengths were also observed [4, 5].

The energy gaps in the ground state bands in the even - *A* Xe nuclei indicate a possible O(6)-like structure. However, a real probe to test the relation to the O(6) dynamical symmetry are the electromagnetic properties of the nuclei. In particular, one can emphasize the importance of the electric quadrupole moments which vanish within the γ-soft framework.

Previous studies provide experimental information about transition strengths in the even-*A* Xe nuclei but the information about quadrupole moments is sparse [4–9]. The present work reports results from measurements of the electromagnetic properties of ^{126,128}Xe, with focus on the quadrupole moments of several excited states.

2 Experimental Details and Data Analysis

A sub-barrier Coulomb excitation experiment was performed at the National Superconducting Cyclotron Laboratory (NSCL) ReA3 facility (stand-alone mode), Michigan State University (MSU). ^{126,128}Xe nuclei were accelerated to energies of 3.74 MeV/nucleon and 3.81 MeV/nucleon, respectively, and were impinged on a ^{208}Pb target with a thickness of 0.92 mg/cm^2 and a ^{196}Pt target with a thickness of 1.59 mg/cm^2 in separate experimental runs. The beam intensity was on average $\sim 3\times10^5$ pps for ^{128}Xe and $\sim 2\times10^5$ pps for ^{126}Xe.

*e-mail: kisyov1@llnl.gov
**Presnt address: TRIUMF, Vancouver, British Columbia V6T 2A3, Canada

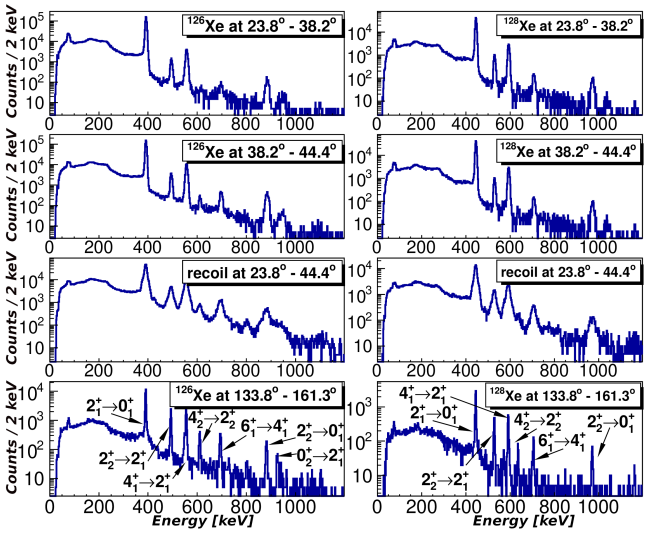

Figure 1. Doppler-corrected spectra of γ-rays detected in coincidence with Xe and recoil target nuclei registered in the Si detector within 4 different angle ranges. Data from runs with a ^{208}Pb and beams of (left) ^{126}Xe and (right) ^{128}Xe are displayed.

The scattered nuclei and the γ-rays following the Coulomb excitation were detected using the Joint Array for NUclear Structure (JANUS) [10] setup. The configuration consisted of a pair of segmented Micron S3-type double-sided Si detectors (Bambino2) and the Segmented Ge Array (SeGA) [11] (comprising of sixteen 32-fold segmented high-purity germanium detectors with cylindrical crystals).

The experimental data were sorted and processed using the GRUTinizer software. The setup arrangement allowed to split the Si detectors data in 4 datasets for each of the studied Xe nuclei and construct Doppler-corrected SeGA γ-ray distributions for each of them. Spectra from such datasets with a ^{208}Pb target are presented in Fig. 1. Partial level schemes of ^{126,128}Xe are shown in Fig. 2. The transitions observed in the present work highlighted in red.

The efficiency corrected experimental γ-ray yields were compared to calculations performed with the semi-classical Coulomb excitation code, GOSIA [12, 13], and electromagnetic properties of the nuclei were extracted. The $<2_1^+||E2||0_1^+>$ matrix elements in both nuclei were first determined using the ^{196}Pt target datasets and a GOSIA2/GOSIA iterative analysis procedure [14, 15], as described in [16]. Full sets of transition and diagonal matrix elements were futher obtained in a standard GOSIA χ^2 minimization with both target datasets for each nucleus.

Known literature data for branching ratios, mixing ratios, and lifetimes were used in addition to the present experimental γ-ray yields during the minimization procedures (Table 1).

3 Experimental Results and Discussion

Experimental results for transition matrix elements and $B(E2)$ values determined in the current work are presented in Table 2, along with a comparison to theoretical values

Table 1. Experimental branching ratios (BR), $E2/M1$ mixing ratios (δ), and lifetimes (τ) in ^{126,128}Xe known prior to the present work [6, 17–20]. These values were used during the GOSIA χ^2 minimizations.

^{126}Xe				
J_i^π	J_f^π	E_γ [keV]	BR	δ
2_2^+	2_1^+	491	1	+9.1 (+43 -23)
2_2^+	0_1^+	880	0.2541 (19)	
4_2^+	2_2^+	608	1	
4_2^+	2_1^+	1099	0.211 (3)	
4_2^+	4_1^+	546	0.504 (5)	+3.0 (+10 -9)
^{128}Xe				
J_i^π	J_f^π	E_γ [keV]	BR	δ
2_2^+	2_1^+	526	1	+4.4 (7)
2_2^+	0_1^+	969	0.268 (5)	
4_2^+	2_2^+	635	1	
4_2^+	2_1^+	1161	0.361 (10)	
4_2^+	4_1^+	571	0.772 (19)	+1.9 (+3 -5)
J^π		E [keV]		τ [ps]
2_1^+		443		26.8 (3)
4_1^+		1033		4.8 (2)
6_1^+		1737		1.8 (2)
2_2^+		969		8.7 (5)
4_2^+		1604		3.5 (2)

and previous measurements. The uncertainties of the experimental values were obtained by taking into account all correlations between the matrix elements.

The experimental diagonal matrix elements, and the respective quadrupole moments, determined in the GOSIA χ^2 minimizations are presented in Table 3, along with a comparison to theoretical calculations.

The new experimental results for the transition strengths in ^{126,128}Xe are in general in a good agreement with literature values. Although the experiemntal $B(E2; 2_1^+ \rightarrow 0_1^+)$ = 56 (5) W.u. for the decay of the first 2^+ state in ^{126}Xe differs from the evaluated data in Ref. [17, 21], it agrees well with recently performed measurements [22–24]. The newly determined quadrupole moments suggest deviations from the O(6)-like structure in the ground state bands. The low magnitude of the quadrupole moments of the 2_2^+ states in both nuclei are notable. These values are consistent in a systematic way with results from measurements in ^{130}Xe [9].

Schematic claculations within the asymmetric rotor approach [1] were performed for ^{126,128}Xe. The triaxiality parameters γ were determined from the experimental features of the second 2^+ states. Transition strengths were calculated based on the model predictions for the respective values of γ, with a normalization to the experimental $<2_1^+||E2||0_1^+>$ values applied (Table 2 and 3).

A mode detailed theoretical approach was applied using microscopic shell model calculations. The model employs a realistic Hamiltonian (called PMMU) which combines the pairing plus multipole terms with the monopole interaction obtained by the monopole based universal force [25]. It has been proven to describe well energy spectra and electromagnetic transitioins in a wide range of nuclei [26, 27]. The present PMMU calcula-

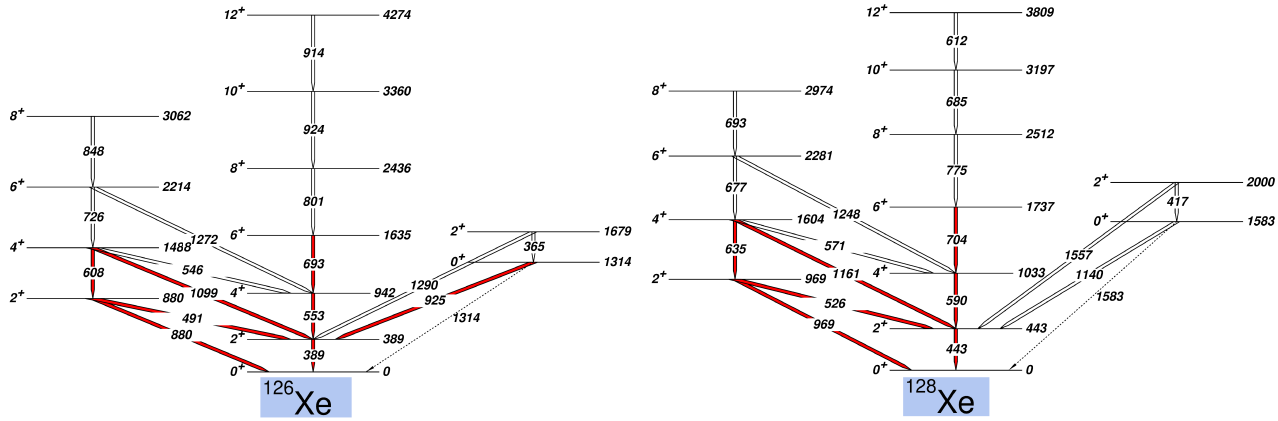

Figure 2. Partial level schemes of ^{126,128}Xe. The data were taken from [6]. The transitions observed in this work are marked in red.

Table 2. Experimental transition matrix elements and $B(E2)$ values in ^{126,128}Xe obtained in the present work. The values are compared to previuos results and theoretical calculations within the asymmetric rotor model and the PMMU shell model.

				^{126}Xe				
J_i^π	J_f^π	$<J_i^\pi\|\|E2\|\|J_f^\pi>_{exp}$ [eb]	$B(E2)_{exp}$ [W.u.]	$<J_i^\pi\|\|E2\|\|J_f^\pi>_{PMMU}$ [eb]	$B(E2)_{PMMU}$ [W.u.]	$B(E2)_{DF}$ [W.u.]	$B(E2)^a$ [W.u.]	
2_1^+	0_1^+	1.03 (4)	56 (5)	0.99	51	56	41.0 (13)	
4_1^+	2_1^+	1.48 (4)	65.1 (34)	1.63	77	79	71.0 (67)	
6_1^+	4_1^+	2.07 (9)	88 (8)	2.13	91	99	84 (11)	
2_2^+	2_1^+	1.00 (4)	54 (4)	0.96	48	57	43.2 (26)	
2_2^+	0_1^+	0.119 (9)	0.75 (11)	0.125	0.82	1.76	0.63 (7)	
4_2^+	2_2^+	0.97 (6)	27.6 (34)	1.31	50	26	36.1 (42)	
0_2^+	2_1^+	0.12 (4)	3.9 (29)	0.15	5.8		5.9 (9)	
				^{128}Xe				
J_i^π	J_f^π	$<J_i^\pi\|\|E2\|\|J_f^\pi>_{exp}$ [eb]	$B(E2)_{exp}$ [W.u.]	$<J_i^\pi\|\|E2\|\|J_f^\pi>_{PMMU}$ [eb]	$B(E2)_{PMMU}$ [W.u.]	$B(E2)_{DF}$ [W.u.]	$B(E2)^b$ [W.u.]	$B(E2)^c$ [W.u.]
2_1^+	0_1^+	0.940 (15)	46.1 (15)	0.92	44	46.1	47 (5)	42.6 (64)
4_1^+	2_1^+	1.38 (4)	55.4 (32)	1.51	66	65	60 (6)	63.5 (52)
6_1^+	4_1^+	1.95 (12)	76 (10)	2.00	80	82	79 (8)	106 (13)
2_2^+	2_1^+	0.92 (4)	44 (4)	1.02	54	46	49 (5)	50.1 (97)
2_2^+	0_1^+	0.105 (8)	0.58 (9)	0.068	0.24	1.56	0.63 (5)	0.65 (8)
4_2^+	2_2^+					21	29 (5)	29.6 (29)

[a] From Ref. [5] [b] From Ref. [7] [c] From Ref. [4]

Table 3. Experimental diagonal matrix elements and quadrupole moments in ^{126,128}Xe determined in the present work. A comparison to theoretical predictions within the asymmetric rotor model (given that the sign of $Q(2_1^+)$ is negative) and the PMMU shell model are presented.

		^{126}Xe		
J^π	$<J^\pi\|\|E2\|\|J^\pi>_{exp}$ [eb]	Q_{exp} [eb]	Q_{PMMU} [eb]	Q_{DF} [eb]
2_1^+	-1.0 (2)	-0.76 (15)	-0.57	-0.52
4_1^+	-0.78 (16)	-0.59 (12)	-0.69	-0.30
2_2^+	+0.14 (9)	+0.11 (7)	+0.51	+0.52
		^{128}Xe		
J_i^π	$<J^\pi\|\|E2\|\|J^\pi>_{exp}$ [eb]	Q_{exp} [eb]	Q_{PMMU} [eb]	Q_{DF} [eb]
2_1^+	-0.58 (-15 +12)	-0.44 (-12 +9)	-0.37	-0.49
4_1^+	-1.38 (13)	-1.04 (10)	-0.45	-0.28
2_2^+	+0.01 (-10 +9)	+0.008 (-0.08 +0.07)	+0.33	+0.49

tions adopt a large model space including $1g_{9/2}$, $1g_{7/2}$, $2d_{5/2}$, $2d_{3/2}$, $3s_{1/2}$, $1h_{11/2}$, $2f_{7/2}$ (referred to as $gdshf$). Conventional shell-model techniques cannot be used with such a large model space. Thus, the recently developed Hartree-Fock-Bogoliubov plus generator coordinate method (HFB+gcm) [28] was applied. It uses the HFB method to generalize a suitable mean field and applies the gcm calculation to obtain the wave functions through superimposing many configurations in the quadrupole-deformation plane.

The present PMMU shell-model calculations for ^{126,128}Xe were performed using the same HFB+gcm code as in Ref. [29], with the same parameters as in Ref. [30]. A comparison between the PMMU level energies and experimental data is shown in Fig. 3. Transition probabilities and quadrupole moments were calculated (with effective charges taken as $e_p = 1.0e$ and $e_n = 0.4e$) and are presented in Tables 2 and 3. A good agreement with the experimental values is observed, except for the quadrupole moments of the 2_2^+ states. It is remarkable that

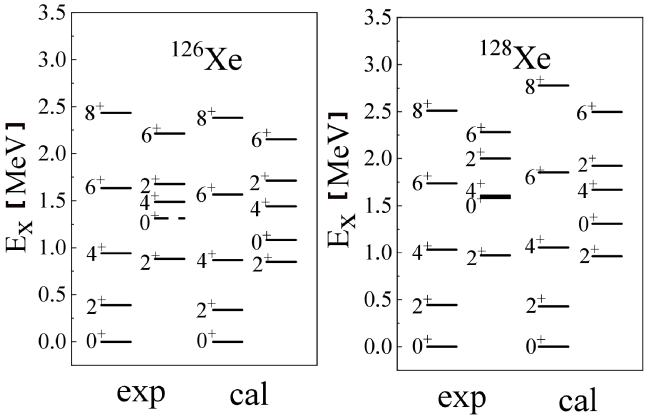

Figure 3. A comparison between experimental energy levels and the predictions within the PMMU shell model for ^{126,128}Xe.

the model calculations reproduce well the small experimental $B(E2; 2_2^+ \rightarrow 0_1^+)$ in ^{126}Xe and ^{128}Xe. The γ-soft model predicts a small $B(E2)$ value for this transition, consistent with this experimental data. The DF γ-rigid calculations could not reproduce this experimental value.

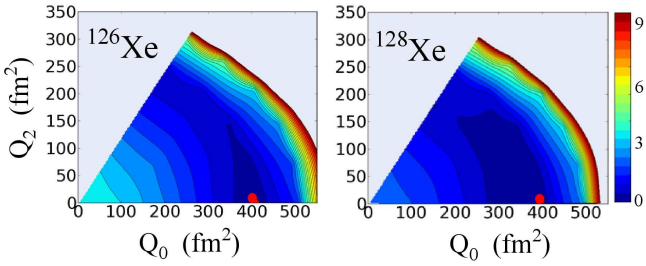

Figure 4. Potential energy surfaces for ^{126,128}Xe.

Fig. 4 shows the potential energy surfaces for ^{126,128}Xe as a function of the quadrupole moments Q_0 and Q_2. The plots suggest very soft energy surfaces for a wide area in the parameter plane. Perturbations can easily drive the nucleus moving in the Q_0-Q_2 plane. Thus, the nuclei can have a variety of possibilities to develop different shapes (including unusual ones) once they get excited.

4 Summary

The electromagnetic properties of ^{126,128}Xe were studied in sub-barrier Coulomb excitation measurements performed at NSCL, MSU. Transition and diagonal matrix elements were determined and compared to theoretical calculations within the schematic γ-rigid asymmetric rotor model and the microscopic PMMU shell model. The experimental results are in a reasonable agreement with the model predictions. The theoretical approaches do not reproduce well the low-magnitude experimental quadrupole moment of the 2_2^+ states, resulting in difficulties to interpret the structure of the nuclei in the γ-bands.

This work was performed under the auspices of the U.S. Department of Energy by Lawrence Livermore National Laboratory under contract DE-AC52-07NA27344.

The work was supported by US DOE Contract No. 89233218CNA000001, and by the U.S. DOE, Office of Science, Office of Nuclear Physics, under Grant No. DE-SC0020451, the US National Science Foundation (NSF) under Grant No. PHY-1565546, and by the DOE National Nuclear Security Administration through the Nuclear Science and Security Consortium, under Award No. DE-NA0003180. YS was supported by the National Natural Science Foundation of China under Contract No. U1932206. KK and NS were supported by the Multidisciplinary Cooperative Research Program in CCS, University of Tsukuba (xg18i035, wo22i002). JH acknowledges support at the under UKRI Future Leaders Fellowship MR/T022264/1.

References

[1] A. S. Davydov and G. F. Filippov, Nuclear Physics **8**, 237 (1958)
[2] L. Wilets and M. Jean, Phys. Rev. **102**, 788 (1956)
[3] R. M. Clark *et al.*, Phys. Rev. C **69**, 064322 (2004)
[4] L. Coquard *et al.*, Phys. Rev. C **80**, 061304(R) (2009)
[5] L. Coquard *et al.*, Phys. Rev. C **83**, 044318 (2011)
[6] NNDC data base, www.nndc.bnl.gov.
[7] J. Srebrny *et al.*, Nuclear Physics A **557**, 663c (1993)
[8] C. Fransen *et al.*, Journal of Physics: Conference Series **205**, 012043 (2010)
[9] L. Morrison *et al.*, Phys. Rev. C **102**, 054304 (2020)
[10] E. Lunderberg *et al.*, NIM A **885**, 30 (2018)
[11] W. F. Mueller *et al.*, NIM A **466**, 492 (2001)
[12] T. Czosnyka, D. Cline, and C. Y. Wu, Bull. Am. Phys. Soc. **28**, 745 (1983)
[13] D. Cline, T. Czosnyka, A. B. Hayes, P. Napiorkowski, N. Warr, and C. Y. Wu, Gosia manual, Version: May 10, 2012
[14] L. P. Gaffney, https://github.com/lpgaff/chisqsurface
[15] J. Henderson, https://github.com/jhenderson88/GOSIAFitter
[16] M. Zielińska *et al.*, EPJ A **52**, 99 (2016)
[17] J. Katakura and K. Kitao, Nucl. Data Sheets **97**, 765 (2002)
[18] Z. Elekes and J. Timar, Nucl. Data Sheets **129**, 191 (2015)
[19] W. Rother, *et al.*, NIM A **654**, 196 (2011)
[20] T. Konstantinopoulos *et al.*, HNPS Advances in Nuclear Physics **18**, 7 (2010)
[21] H. Iimura *et al.*, Nucl. Data Sheets **180**, 1 (2022)
[22] O. Stuch, Ph.D. Thesis, University of Cologne, unpublished (1997)
[23] A. Gade *et al.*, Nuclear Physics A **665**, 268 (2000)
[24] W. F. Mueller *et al.*, Phys. Rev. C **73**, 014316 (2006)
[25] T. Otsuka *et al.*, Phys. Rev. Lett. **104**, 012501 (2010)
[26] K. Kaneko *et al.*, Phys. Rev. C **89**, 011302(R) (2014)
[27] K. Kaneko *et al.*, Phys. Rev. C **92**, 044331 (2015)
[28] N. Shimizu *et al.*, Phys. Rev. C **103**, 064302 (2021)
[29] N. Shimizu, HFB+gcm code, unpublished (2019)
[30] K. Kaneko *et al.*, Phys. Rev. C **103**, L021301 (2021)